DESIGN, ANALYSIS AND CHARACTERIZATION OF THE RF CAVITY FOR THE GYROTRONS

4.1 Introduction

4.2 Synthesis of the Gyrotron Interaction Structure

    4.2.1   Synthesized parameters

    4.2.2   Other essential device operational parameters

    4.2.3   Operating mode selection

4.3 Generalized Nonlinear Analysis of the Gyrotron

    4.3.1   Estimation of RF output power and efficiency

4.4 Electron Beam and RF Wave Interaction Simulation

    4.4.1   Validation with the generalized nonlinear analysis

4.5 Experimental Characterization

    4.5.1   Destructive method

    4.5.2   Non-destructive horn antenna method

    4.5.3   Non-Destructive external adaptor method

4.6 Design of the RF Interaction Cavity for the 28 GHz Gyrot

4.7 Conclusion

4.1　Introduction

The RF power growth in the gyrotron occurs due to the effective interaction between the electromagnetic waves in the TE mode and the gyrating electron beam present in the RF interaction cavity. The annular helically gyrating electron beam is generated with the help of the magnetron injection gun (MIG) and transported to the interaction structure under the influence of both the electric and magnetic fields. The TE mode is naturally present in the RF interaction structure, called cavity due to its resonance behavior. There are variants of the RF cavities used in the gyrotrons for low frequency, low power to high frequency, high power regimes, such as, simple cylindrical cavity, co-axial cavity, complex cavity, confocal cavity, photonic band gap cavity, etc. [Basu (1996), Correa *et al*. (1993), Dumbraj *et al*. (2004), Hu *et al*. (1998), Kern (1996), Piosczyk *et al*. (2003), Sheng *et al*. (2006), Srigiri *et al*. (2001), Vlasov *et al*. 1976), Whaley (1994), Yong *et al*. (1997)]. However, in the conventional gyrotron oscillator, a three section cylindrical cavity is used. Three sections of a gyrotron cavity consist of the uniform middle section serving as the RF power growth region, the down-taper section at one the input side serving as the cut-off region to restrict the RF propagation towards the electron beam source while the third section toward the output side is up-taper section serving as the RF propagating region which converts standing waves into the travelling wave for the RF power extraction out from the cavity. The down-taper section is normally called as the input section and the up-taper section is called as the output section.

The prime objectives in the optimization of the RF interaction cavity parameters are the achievement of the high efficiency and output RF power performance. Design of a gyrotron cavity needs the initial estimation of cavity geometry, particularly the operating mode selection, the middle section dimension where RF signal grows, the RF power growth estimation, etc. Thus, Sections 4.2 presents the initial estimation of cavity and electron beam parameters as well as the operating mode selection through the synthesis process. Then, a generalized nonlinear theory of the gyrotron is discussed with the objective of estimation of the device RF output power, efficiency, etc. (Section 4.3). The electron beam and RF wave interaction through PIC simulation is presented for the optimization of the RF interaction cavity and also validated with the results obtained from the nonlinear analysis (Section 4.4). The experimental characterization of the cold (in absence of the electron beam) cavity performance is finally elaborated in Section 4.5. It may be interesting to explore the design of another frequency gyrotron with the use of the

59

electron beam parameters of a 42GHz gyrotron. In this respect, design of the RF interaction cavity for use in a 28GHz gyrotron is also carried out and presented in Section 4.6 of the present Chapter 4.

4.2 Synthesis of the Gyrotron Interaction Structure

The RF signal growth depends upon the cavity and helically gyrating electron beam parameters. The TE mode used for the interaction has many radial maxima depending upon the selected mode profile and thus, the gyrating electron beam must be launched at the maxima position of the electric field intensity inside the designed middle section of the cylindrical cavity for the effective electron beam and RF wave interaction. Obviously, therefore, the interaction and the gyrating electron beam parameters are important, which are to be estimated and optimized. There are various parameters for these two basic constituents, such as, operating mode, quality factor, start oscillation current, coupling coefficient, etc. for the interaction structure normally known as cavity and magnetic field, beam voltage, beam current, etc. for the gyrating electron beam. Out of these parameters, some of the parameters are independent and some depends upon both the RF cavity as well as the electron beam.

4.2.1 Synthesized parameter

For the interaction structure, that is, RF cavity radius can be obtained from (1.5) as

$$ r_{cav} = \chi'_{m,n} \frac{\lambda_0}{2\pi} \tag{4.1} $$

where $\chi'_{m,n}$ is the nth root of derivative of the Bessel function of mth order and first kind. In case of a particular $TE_{m,n}$ mode, the suffix m and n are the azimuthal and radial index numbers, respectively. Here, the radial index defines the maxima position of the TE mode. The magnetic field required for the gyration of the electron beam can be obtained from (2.6). The beam voltage is initially selected through estimation of the relativistic mass factor (γ_o) in terms of the beam voltage (V_b) through (2.7). The beam current then can be easily estimated for the desired output power (P_o) and the applied DC beam voltage (V_b) of the device. The electron beam launching radius can be obtained from (2.8) through (4.1).

The RF power growth occurs in the middle section of a gyrotron cavity. The length of middle section (L) is important for proper growth and its optimization is directly related to the

quality factor of the cavity. The quality factor (Q) is a very important physical parameter to describe the oscillatory behavior of any device and given by the following relation related with the resonant frequency (f):

$$Q = 2\pi \frac{Energy\ stored}{Energy\ dissipated\ per\ cycle} = 2\pi f \frac{Energy\ stored}{Power\ loss} .$$

(4.2)

The quality factor (Q) is related with the diffractive quality factor (Q_{diff}) and the ohmic quality factor (Q_{ohm}) through the expression given as:

$$\frac{1}{Q} = \frac{1}{Q_{diff}} + \frac{1}{Q_{ohm}} ,$$

(4.3)

where the diffractive quality factor Q_{diff} can be defined as the power loss from the middle section of the cavity due to the RF propagation through the output taper section. The time (τ) for energy to travel out of the cavity determines the diffractive quality factor and is related to the minimum diffractive quality factor as:

$$Q_{diff,min} = \omega\tau = \omega\frac{L}{v_g} = 4\pi\left(\frac{L}{\lambda}\right)^2 ,$$

(4.4)

where $Q_{diff,\ min}$, ω, v_g, λ and L are the minimum diffractive quality factor, the angular frequency of RF, the group velocity, the RF wavelength and the length of middle section of interaction cavity, respectively. The interaction cavity middle section is extended on both sides in terms of the input and the output tapers and thus the reflections occur from both the sides to the middle section. The reflections at both the ends are necessary for formation of standing wave in the RF interaction cavity. The actual diffractive quality factor becomes somewhat different due to the reflections at both the ends of middle section and is modified as [Woskoboinikow *et al.* (1987)]:

$$Q_{diff} = \frac{Q_{diff,min}}{1-\rho} = \frac{4\pi}{(1-\rho)}\left(\frac{L}{\lambda}\right)^2 .$$

(4.5)

Here, ρ is the combined reflection at both the ends of middle section ($\rho = R_{in}, R_{out}, R_{in}$ and R_{out} are the reflections at both ends, that is, input and output ends). Other major RF loss in the interaction cavity is due to the finite conductivity of the cavity material (oxygen free high conductivity (OFHC) copper) and expressed in terms of the ohmic quality factor. The ohmic quality factor directly depends on the material electrical properties (in terms of the skin depth) and the electric field pattern (TE mode). The expression for the ohmic quality factor is given as

61

$$Q_{ohm} = \frac{R_c'}{\delta}\left[1 - \frac{m^2}{\chi_{m,p}'^2}\right]$$
(4.6)

where δ is the skin depth and R_c' is resistance of the cavity.

Another important parameter for the gyrotron operation is the start oscillation current (SOC) which is defined as the minimum current required for the gyrotron to start oscillation. Thus, when the beam current exceeds the start oscillation current, the self-excitation conditions are fulfilled and this gives rise to the device oscillations. The expressions of start oscillation current obtained from self-consistent analysis, can be written as [Kartikeyan *et al.* 2004)]:

$$I_{st} = (1.68\times10^4)\frac{\gamma_o I_{stN}}{Q}\beta_\perp^4\frac{L}{\lambda_0}\frac{\left(\chi_{m,n}'^2 - m^2\right)J_m^2(\chi_{m,n}')}{J_{m\pm1}^2\left(k_\perp R_b\right)}$$
(4.7)

$$I_{stN} = \left(\frac{4}{\pi\mu^2}\right)\left[\frac{e^{2x^2}}{\mu x - 1}\right] \quad \text{and} \quad x = \mu\Delta/4$$

$$k_\perp = \chi_{m,n}'/R_c$$
(4.8)

where $\beta_\perp$ is the normalized transverse electron velocity, $J_m(x)$ refers to the Bessel function of first kind of order m and argument x.

To avoid the excitation of competing mode, proper launching of the electron beam is very necessary. The electron beam parameter known as the coupling coefficient provides information about the beam launching position and its tolerance. The coupling coefficent should be maximum for the selected mode, so that the desired mode can be excited during the gyrotron operation. The expression for coupling coefficent is given as [Kartikeyan *et al.* (2004)]:

$$CC = \frac{J_{m\pm1}^2\left(k_\perp R_b\right)}{\left(\chi_{m,n}'^2 - m^2\right)J_m^2(\chi_{m,n}')} \quad .$$
(4.9)

4.2.2 Other essential device operational parameters

The operating mode selection depends upon the RF interaction cavity and gyrating electron beam as discussed in the previous section. However, there are some more essential device operational parameters, such as, cavity wall loading, voltage depression and limiting current should also be estimated. Then, these parameters have to be set within the well defined technical criteria limit, such as, ohmic wall loss (kW/cm^2) < 2.0, voltage depression (kV) < 10%

of beam voltage and limiting current (A) > 200% of the total beam current. These technical parameters are discussed below.

Ohmic wall loss: Some of the electromagnetic power in the interaction cavity is dissipated in the form of ohmic heating due to the finite conductivity of the cavity material. The ohmic wall loss (heat dissipated per unit area) (dP/dA) can be calculated from the formula [Kartikeyan *et al*. (2004), Singh (2012)]:

$$\frac{dP}{dA} = 2\pi \sqrt{\frac{1}{\pi Z_0 \sigma}} \left(\frac{PQ}{L\lambda^{3/2}} \right) \left(\frac{1}{\chi_{mp}'^2 - m^2} \right) \quad , \tag{4.10}$$

where σ and Z_0 are the electrical conductivity of cavity material and the free space impedance, respectively. The practical ohmic wall loss is around 1.25 multiple of the ohmic wall loss calculated through (4.6), due to higher conductivity at the operating condition and surface roughness which increases the RF-skin-losses [Kartikeyan *et al*. (2004), Singh (2012)].

Space charge parameters: The space charge effect caused due to the potential of the transported charge beam and critically depends on the charge transportation geometry and the structure geometry through which the charge is moving. The space charge effect can be defined in terms of the voltage depression (V_d) and the limiting current (I_L). The voltage depression (V_d) and the limiting current (I_L) can be expressed in term of beam current, cavity radius and beam radius as follow [Kartikeyan *et al*. (2004), Singh (2012)]:

$$V_d \approx (60\Omega) \frac{I_b}{\beta_z} \ln\left(\frac{R_c}{R_b} \right) \quad , \tag{4.11}$$

$$I_L \approx 8500\, A [I^* / \ln \frac{R_c}{R_b}] \quad , \tag{4.12}$$

and

$$I^* = \gamma_o \left[1 - \left(1 - \beta_{zo}^2\right)^{1/3} \right]^{3/2} \quad . \tag{4.13}$$

where β_{zo} is the initial value of axial propagation constant (β_z) at the cavity entrance.

4.2.3   Operating mode selection

Different TE modes are found for the possible use in a 42GHz, 200kW gyrotron and then all the relevant mode selection parameters are obtained using the analytical expressions as discussed in sub-section 4.2.2. The results of some typical TE modes for the 42GHz, 200kW

gyrotron are given in Table 4.1. Using the technical criteria for the voltage depression, the limiting current and the wall loading, TE modes have been selected for the possible applications. The estimations of start oscillation current and coupling coefficient have also carried out for all these operating modes using (4.7)–(4.9). The start oscillation current and the coupling coefficient are also estimated for all these modes. From these studies, TE_{03} mode is found as the most suitable operating mode for use in 42GHz, 200kW gyrotron to be developed.

Table 4.1: Mode selection parameters for suitable modes for 42GHz gyrotron cavity.

m	*n*	$\chi'_{m,n}$	r_{cav} (mm)	r_b (mm)	V_d (kV)	I_L (A)	dP/dA (kW/cm^2)
0	2	7.016	7.98	2.09	2.99	29.1	0.104
*0	2	7.016	7.98	6.05	0.51	138.1	0.104
0	3	10.173	11.57	2.09	3.82	22.8	0.049
*0	3	10.173	11.57	6.06	1.44	59.0	0.049
2	1	3.054	3.47	2.09	1.13	76.9	0.958
2	2	6.706	7.62	2.09	2.89	30.1	0.125
2	3	9.969	11.33	2.09	2.89	30.1	0.054
*2	3	9.969	11.33	6.06	1.40	61.0	0.054
4	2	9.282	10.55	4.78	1.77	49.1	0.073
5	2	10.52	11.96	6.05	1.53	57.0	0.060

(* the electron beam is positioned at the 2nd radial maximum of the RF-field)

4.3   Generalized Nonlinear Analysis of the Gyrotron

RF power growth is a nonlinear phenomenon and thus nonlinear analysis is required for the estimation of gyrotron cavity behavior related to the RF power growth. The generalized nonlinear analysis has been briefly presented in the following subsection.

4.3.1   Estimation of the RF output power and efficiency

G. S. Nusinovich developed a generalized nonlinear analysis for the gyrotron in the form of generalized parameters and then later on it was simplified by B. G. Danly and R. J. Temkin. This nonlinear analytical approach is now well established and still relevant for the design of the gyrotron including its RF interaction cavity [Nusinovich (1999)]. This analysis allows the

straight forward design and optimization of the harmonic gyrotron. The variation of energy and electron phase with angle of the electron momentum vector can be expressed in terms of the normalized field amplitude (F), the normalized interaction length (μ) and the normalized magnetic field detuning parameter (Δ) as follows [Nusinovich (1999)]:

$$\frac{du}{d\xi} = 2Ff(\xi)\sin\theta(1-u)^{n/2} \tag{4.14}$$

$$\frac{d\theta}{d\xi} = \Delta - u - nFf(\xi)(1-u)^{\frac{n}{2}-1}\frac{\gamma}{\gamma_o}\cos\theta \tag{4.15}$$

where u, θ, ξ, n, $f(\xi)$, γ and γ_o are the normalized energy, electron phase, normalized axial position, (any) integer, axial field profile, relativistic factor and initial values of γ at the cavity entrance, respectively. Nonlinear analysis is general in nature and used here for the typical 42GHz, 200KW gyrotron and used elsewhere by different researchers for the initial design of gyrotron operating at the various frequencies. Here, it is of interest to discuss the normalization aspects of the these parameters, such as, the normalized field amplitude (F) is the electric field normalized with respect to the magnetic field at cavity. Further, the normalized interaction length (μ) is the normalized length of RF growth region normalized with respect to the wavelength of gyrotron operation. Finally, the normalized magnetic field detuning parameter (Δ) is the mismatch factor and the function of the transverse velocity of electrons. Obviously, the normalized field amplitude is the function of magnetic field and beam radius, the normalized interaction length is the function of cavity middle length and the detuning parameter is the function of transverse velocity of electrons, respectively.

Now, the total interaction efficiency (η) can be given as:

$$\eta = \frac{\beta_{\perp o}^2}{2(1-\gamma_o^{-1})}\eta_\perp \tag{4.16}$$

where $\beta_{\perp o}$ is the normalized transverse velocity of electrons and subscript o denotes the initial value of quantity. Further, the perpendicular interaction efficiency $(\eta_\perp)$ is defined as:

$$\eta_\perp(F,\mu,\Delta) = \langle u(\xi_{out})\rangle_{\theta_o} , \tag{4.17}$$

Here, bracket denotes the average particles energy at the end of interaction cavity. The perpendicular interaction efficiency is a function of these three normalized parameters, namely, the normalized field amplitude (F), the normalized interaction length (μ) and the magnetic field

detuning parameter (Δ). The nonlinear analysis is very handy for calculating the interaction efficiency and the phase space diagram. A computer code has been written in MATLAB based on the generalized nonlinear analysis for the initial design of the interaction cavity. The coupled differential equations (4.14)-(4.15) have been solved by using the Runge-Kutta numerical approach. The normalized parameters are the function of the operating mode, the electron beam parameters and the interaction cavity geometrical parameters. The transverse efficiency contour plots for various detuning factor as a function of normalized field amplitude and normalized interaction length has been obtained by using developed computer code and shown in Figs. 4.1 to 4.4 for a range of transverse interaction efficiency from 0.20 to 0.75. A range of the normalized parameters is obtained for the maximum transverse interaction efficiency (Table 4.2). Out of these ranges, the best transverse interaction efficiency around 65% has been achieved by using the values mentioned in Table 4.1 and then using (4.3) and beam parameters related to beam voltage and beam current. The values of these normalized parameters for the best efficiency have been obtained respectively as F=0.14, μ=10.17 and Δ=0.51 for 42GHz, 200KW gyrotron.

Further, the plots between the normalized energy and the normalized length have been obtained for a number of electrons throughout the length of cavity. Fig. 4.5 exhibits the normalized energy of the electrons with respect to the normalized cavity length and clearly shows that all the electrons have the equal energies at the initial position. However, the electron energies for different electrons are varied after a certain length in the cavity clearly due to exchange of energy from the electron beam to the RF field. Similarly, Fig. 4.6 presents the electron phase plot versus the normalized length for the different electrons. These plots shown in Figs. 4.5 and 4.6 have been used to obtain the transverse interaction efficiency through (4.4). The magnetic field, the cavity RF power growth, length and the electron velocity ratio can be calculated by using these generalized parameters and obtained as 1.615T, 44mm and 1.4, respectively for the 42GHz, 200kW gyrotron. These parameters have been initially used for beam wave interaction simulation for the final optimization of gyrotron cavity (Section 4.4).

Table 4.2: Optimized generalized parameters range for maximum transverse efficiency (>70%).

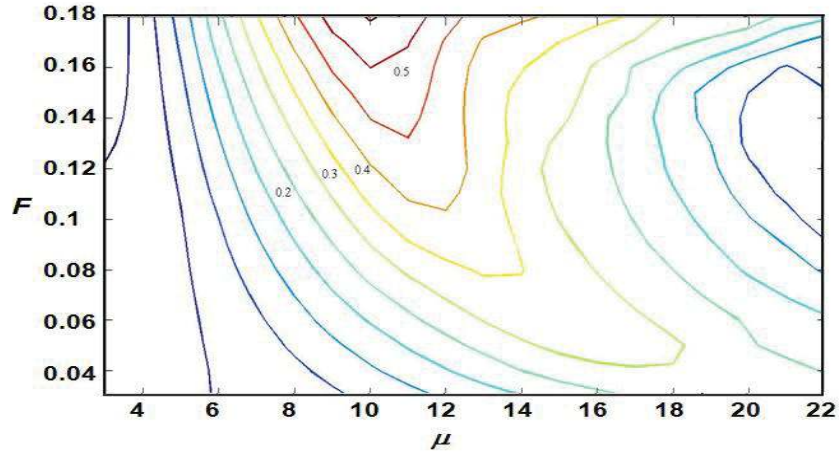| Parameter	Range
Generalized field amplitude (F)	0.11-0.17
Generalized length (μ)	10-17
Detuning factor (Δ)	0.3-0.5

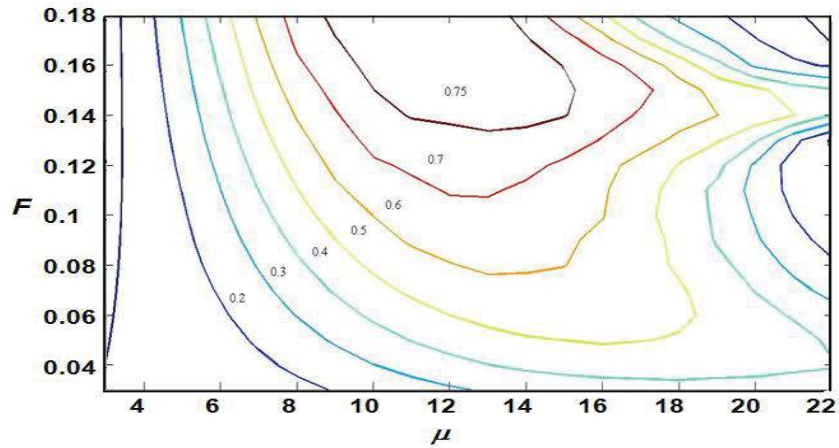**Fig. 4.1:** Transverse efficiency contour plot as a function of *F* and *μ* for *Δ*=0.1 '

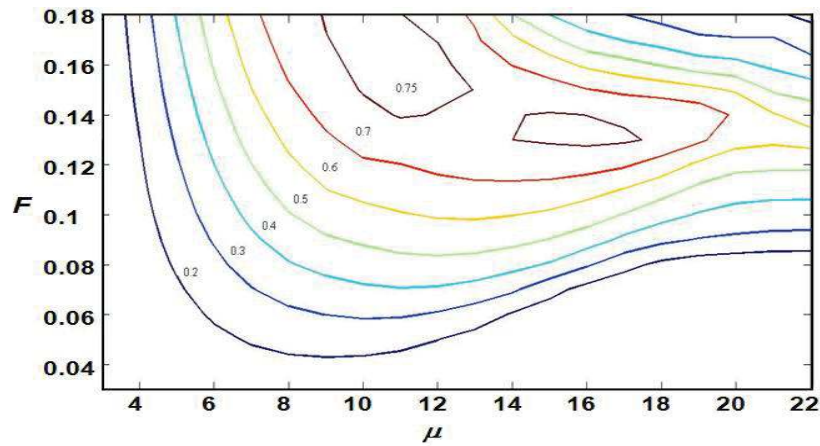**Fig. 4.2:** Transverse efficiency contour plot as a function of *F* and *μ* for *Δ*=0.3.

Fig. 4.3: Transverse efficiency contour plot as a function of *F* and *μ* for (c) *Δ*=0.5.
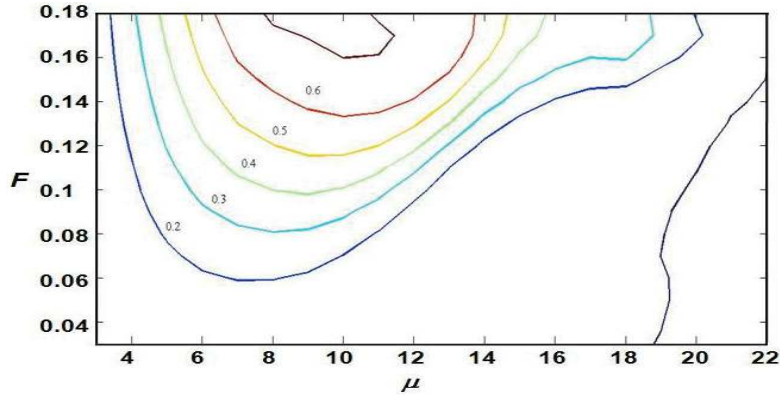
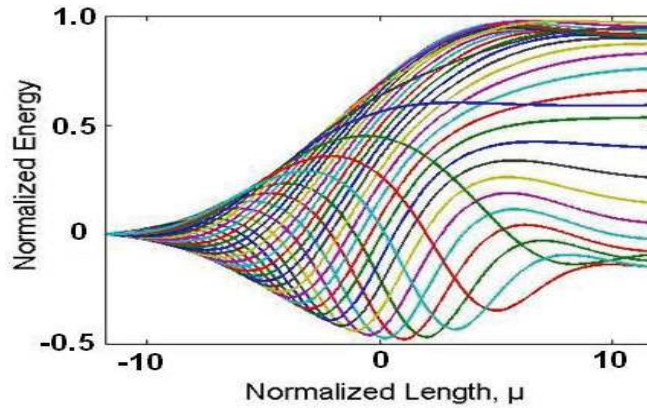**Fig. 4.4:** Transverse efficiency contour plot as a function of F and μ for $\Delta=0.6$.

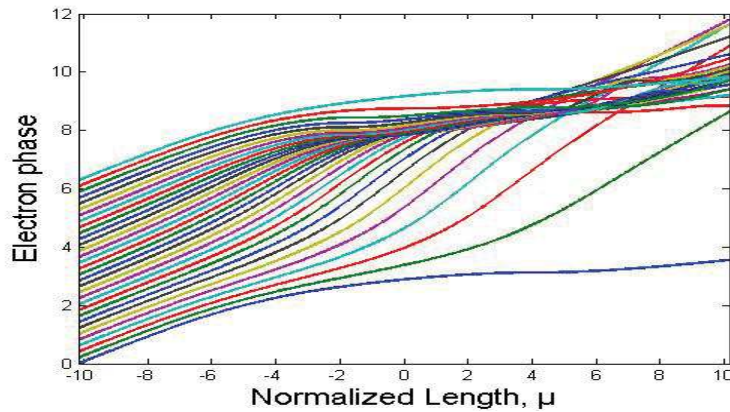**Fig. 4.5:** Normalized energy versus normalized length for 42 GHz gyrotron cavity.

Fig. 4.6: Normalized length versus electron phase plot for 42 GHz gyrotron cavity.

4.4 Electron Beam and RF Wave Interaction Simulation

The gyrotron RF interaction cavity is normally a three section cavity. The various cavity parameters such as operating mode, cavity middle section, i.e., active interaction region, as well as electron beam parameters, such as, operating mode, beam launching position, magnetic field, radius and length of cavity middle section length, etc. have been obtained through the synthesis

68

process. The beam-wave interaction simulation has been carried out using a commercial PIC code MAGIC to the final optimization of cavity and the electron beam parameters and the design of complete cavity including both down-taper and up-taper sections [MAGIC (2007)]. Figs. 4.7 and 4.8 show the typical contour plots of the TE_{03} operating mode. The frequency and power growth results obtained from MAGIC clearly show that at 42GHz frequency ~275kW power is generated and the typical results are presented in Figs. 4.9 and 4.10. In this beam-wave interaction simulation, the complete geometry of the RF interaction structure is optimized including both the input and output taper sections. Table 4.3 shows the optimized geometry of the interaction structure for the 42GHz, 200kW gyrotron. The sensitivity analyses of various parameters are also carried out to fix the fabrication tolerance, but, however, not presented here for the sake of briefness.
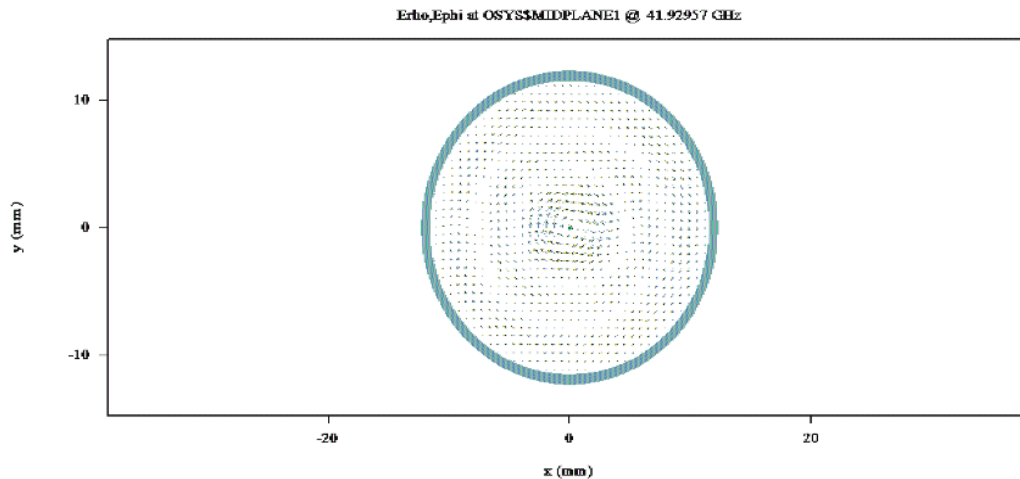

Fig. 4.7: Vector plot of the electric field profile at top cross sectional view.
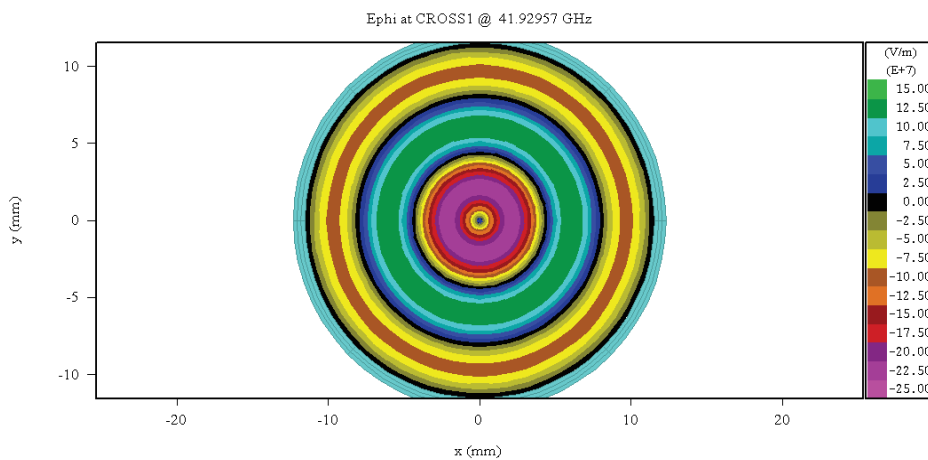

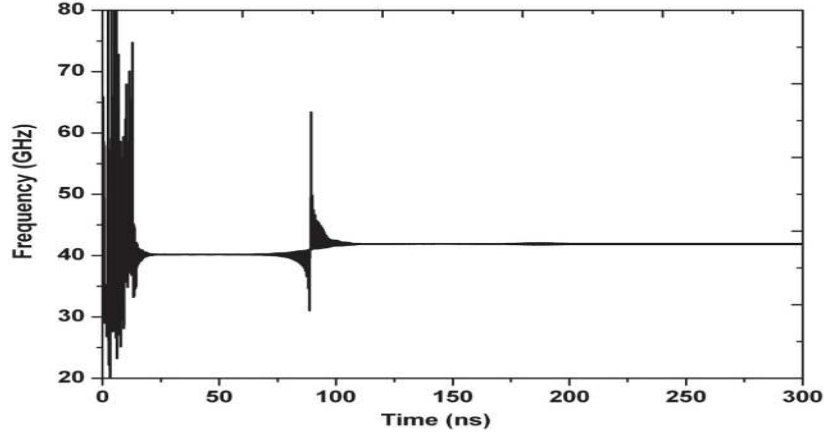**Fig. 4.8:** Contour plot of the electric field profile at top cross sectional view.

Fig. 4.9: Frequency growth with respect to time (V_b=65 kV, I_b=10 A, B_0=1.61 T, α=1.3).
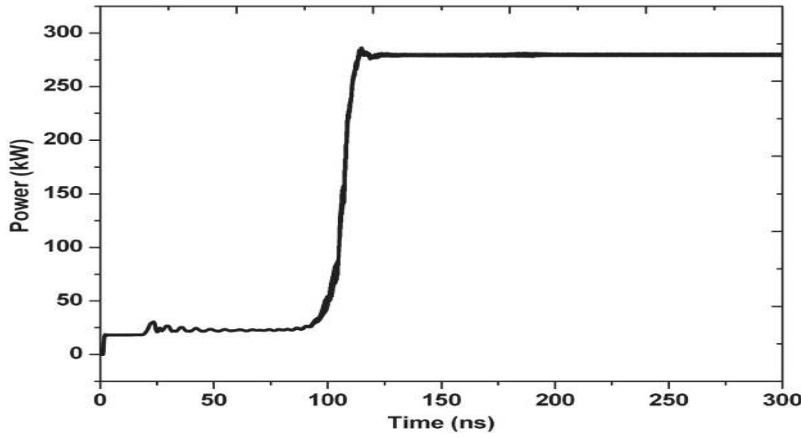

Fig. 4.10: RF Power growth with respect to time (V_b=65 kV, I_b=10 A, B_0=1.61 T, α=1.3).

Table 4.3: Optimized 42GHz gyrotron interaction cavity parameters.

Parameter	Value
Middle section length (L)	44 mm
Middle section radius (R_c)	11.55 mm
Input taper length (L_1)	30 mm
Output taper length (L_2)	46 mm
Input taper angle (θ_1)	2°
Output taper angle (θ_2)	3°

4.4.1 Validation with the generalized nonlinear analysis

Figs. 4.11 to 4.13 present the comparisons between the analytical and simulated results for the gyrotron interaction cavity for the typical selected parameters, namely, cavity magnetic field =1.615T, beam voltage = 65kV, beam current =10A, electron beam velocity ratio = 1.4 and

RF cavity middle section length = 44mm. It is of interest to mention that the analytical results are obtained from the generalized nonlinear analysis (Section 4.3) and the simulated results are obtained using MAGIC code (Section 4.4). From these Figs. 4.11 to 4.13, it is clear that both analytical and simulated results are matching well with the middle section of the gyrotron RF interaction cavity.
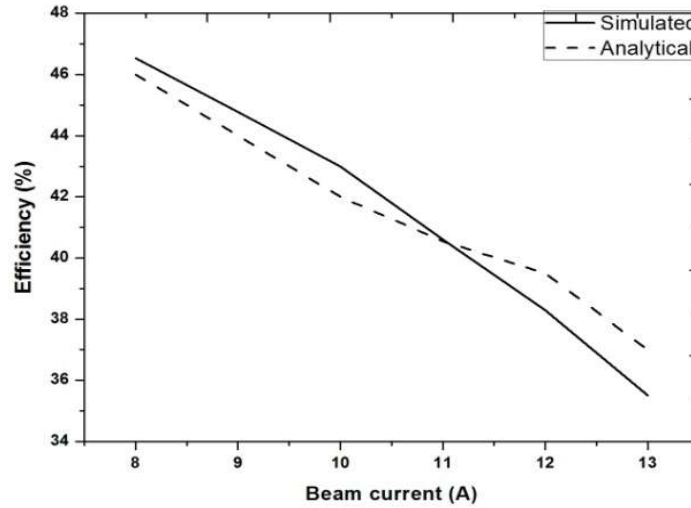

Fig. 4.11: Efficiency Versus beam current **plot** (cavity magnetic field =1.615T, beam voltage = 65kV, electron beam velocity ratio = 1.4 and cavity middle section length = 44mm).
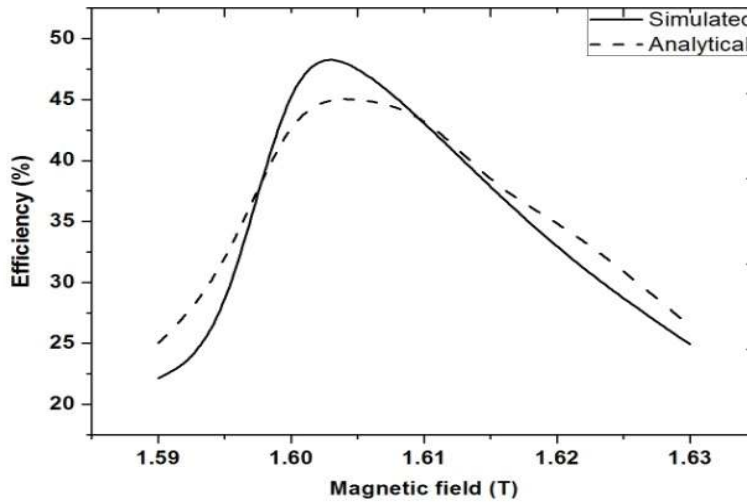

Fig. 4.12: Efficiency versus cavity DC magnetic field plot (beam voltage = 65kV, beam current =10A, electron beam velocity ratio = 1.4, cavity middle section length = 44mm).
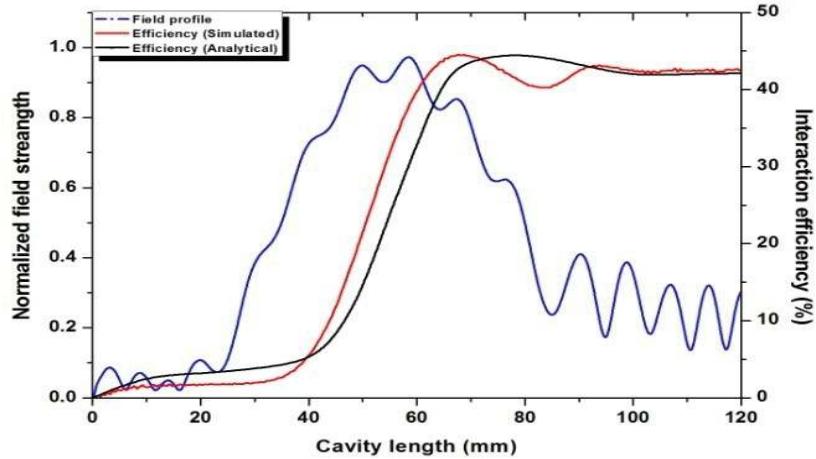
71

Fig. 4.13: Normalized field strength and interaction efficiency versus RF cavity middle section length (analytical and simulated results) (cavity magnetic field =1.615T, beam voltage = 65kV, beam current =10A, electron beam velocity ratio = 1.4).

4.5   Experimental Characterization

The gyrotron performs perfectly if the designed operating mode is excited at the desired frequency. For this purpose, the designed RF interaction cavity is fabricated and then characterized in the cold condition (in the absence of electron beam) related to eigenfrequency, the quality factor and the electric field profile. The RF cavity characterization can be made through both (i) destructive method and (ii) non-destructive method [Barroso *et al.* (1997), Castro *et al.* (2000), Ginzton (1957), Woskoboinikow *et al.* (1987)].

4.5.1   Destructive method

In the destructive method, the desired TE_{0n} mode is excited by passing an electric probe through a hole made in the cavity wall and the power is detected through another electric probe by putting it at the up-taper end of the cavity. The field intensities of the desired mode in the cavity are established by means of an electric probe or loop coupling antenna. The electric probe works as a monopole antenna. The length of the probe is adjusted for the impedance matching between the probe and the central section of the RF resonator. The block diagram of the RF cavity measurement by the perturbation technique is depicted in Fig. 4.14. The standing-wave electric field profile and TE mode pattern are determined by the perturbation method. This method is based on the fact that by introducing the dielectric or metal object inside the cavity, there is a change in the resonant frequency of the RF interaction cavity. After the excitation of the desired mode in the cavity, the eigenfrequency measurement, the loaded quality factor

72

measurement and the mode identification can be performed. The mode identification inside the cavity is done by analyzing the electric field profiles obtained by perturbing the resonant frequency in axial, radial and azimuthal directions, respectively.
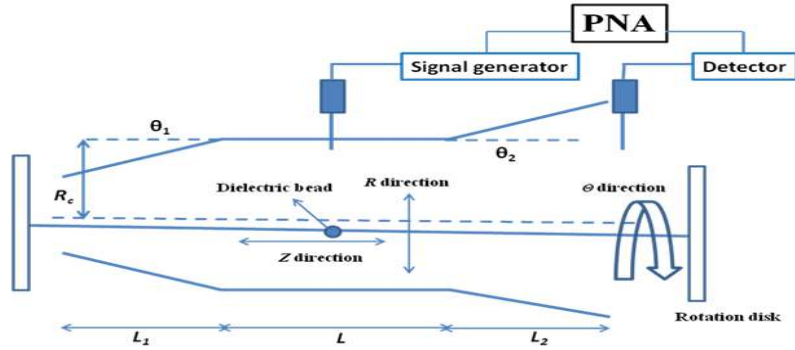

Fig. 4.14: Block diagram of measurement technique by perturbation method (L's; lengths of various cavity sections, R's: radii of various sections).

The presence of dielectric bead causes the perturbation in the electric and the magnetic fields. The change in electric and magnetic field creates a shift in the resonance frequency. The relation between the variations in energy and shift in resonance frequency is given by the Slater-Tischer theorem [Castro *et al.* (2000), Thumm (2011)]:

$$\frac{f - f_0}{f_0} = \frac{\Delta W_E - \Delta W_H}{W_E - W_H} \tag{4.18}$$

where f_0 and f are the unperturbed and perturbed resonant frequencies respectively. (4.18) represents that both the maximum electric (W_E) and magnetic energies (W_H) which are changed by ΔW_E and ΔW_H, respectively. In case of a small dielectric sphere of radius (a) and dielectric constant (ε_r) introduced into the cavity at the axial position z, the corresponding shift in frequency Δf ($= f - f_0$) is given by [Castro *et al.* (2000), Thumm (2011)]:

$$\frac{\Delta f}{f_0} = - \pi a^3 \frac{\varepsilon_r - 1}{\varepsilon_r + 2} \frac{\varepsilon_0 E^2(z)}{\Delta W_E} \tag{4.19}$$

where $E(z)$ is the electric field intensity in the axial direction and ΔW_E is the change in electric energy due to the presence of dielectric bead. The perturbing object is taken small enough so that the electric field is assumed to be uniform over the surface of the object. The shift in frequency is proportional to the square of the electric field at the axial position of dielectric bead as evident from (4.19). A plot of square root of frequency-shift versus axial probe position yields the

longitudinal profile of the electric field. By moving the dielectric bead in various directions (radial, azimuthal and axial), the electric field profile can be plotted in terms of the shifted frequency. The dielectric bead is suspended by a thin nylon thread with a spring arrangement. The dielectric bead can be moved in all three directions, that is, r, Φ and z. The circumferential motion of the nylon thread and consequently the dielectric sphere are adjusted by two graduated discs ($0°$-$360°$). The shift from the unperturbed resonant frequency yields a measure of the electric field intensity at the corresponding axial position. The use of the dielectric sphere of the diameter about $\lambda/10$ wavelength is sufficient for the better result so that a perturbation in frequency can be detected without affecting the total Q.

However, there may be some discrepancy in the above measurement technique due to (i) misalignment of the nylon thread relative to the resonator azimuthal coordinates, (ii) effect of the coupling hole made in the RF cavity and probes as undesired perturbing elements, besides the nylon thread itself, (iii) presence of the dielectric sphere inside the resonator, probably causing the undesired reflections which can slightly change the electric field structure and (iv) occurrence of quasi-stationary wave rather than standing wave field as required by the perturbation technique.

The quality factor Q of the cavity is determined by the -3dB method (half power bandwidth method). In this method, the cavity with input and output terminals is used as a transmission device in the reflection mode. The output signal is measured as a function of frequency, resulting in the conventional resonance curve from which the Q value can be computed by half-power bandwidth method at -3dB point. The loaded quality factor (Q_L), unloaded quality factor (Q_0) and external quality factor (Q_{ext}) of the cavity are given as:

$$Q_L = \frac{f_r}{\Delta f} \quad , \tag{4.20}$$

$$Q_0 = Q_L(1+\beta) \quad , \tag{4.21}$$

and
$$Q_{ext} = \frac{Q_0}{\beta} \quad , \tag{4.22}$$

where β is the coupling coefficient.

Experimental set-up: An experimental set-up for the measurement of electric field profile inside the resonator based on the perturbation method is designed and developed where vector network analyzer (VNA) is used as the RF source (Fig. 4.14). With the help of this set-up, the axial,

radial, azimuthally electric field components are measured to identify the excited mode inside the resonator. The dielectric sphere suspended with a nylon thread can move in r, φ and z directions in this set up. After perturbing the electric field, a plot of square root of frequency shift in resonant frequency versus position of dielectric bead yields the electric field profile. A small size perturbing bead is considered for use so that it does not disturb the field profile inside the cavity and the electric field remains uniform over the dielectric bead. The dielectric bead of the diameter about $\lambda/10$ is used so that a perturbation in resonant frequency can be detected without affecting the cavity quality factor. The experimental results are obtained with the resonators operating at the 42GHz. The field profile of the operating mode are also measured and plotted but, here, due to briefness of manuscript not presented here.

4.5.2 Non-destructive horn antenna method

The cavity is excited by coupling the power from an RF source to the interaction cavity to be characterized for its RF behavior through the horn antenna in the non-destructive horn antenna method. The block diagram for the RF measurement adopting the non-destructive method by using antenna system is shown in Fig. 4.15. In this method, the resonant cavity is excited for the RF signal through a horn antenna and returned power achieved from a mirror is investigated for the microwave measurement of the cavity characteristics. This measurement technique is successively used for the various gyrotron interaction cavity characterizations for its RF behavior and is met most design data of the resonators used in successful gyrotron operations. In this method, the resonator radiation pattern is detected and analyzed for the measurement of the electric field profile for identification of the modes, measurement of the quality factor and resonant frequency for the desired operating mode as well as the presence of other nearby modes. The RF interaction cavity under test is placed in the receiver antenna far field region for detection because of the sensitivity of the receiver and so eliminated any interaction between the cavity under test and the receiver for good resolution.

The cavity is so aligned and oriented so that a peak or null of the resonator mode is detected with a receiver properly. The receiver antenna is further connected with the vector network analyzer (VNA). The alignment of the interaction is adjusted with respect to the horn antenna system, so that maximum coupling can occur between interaction cavity and antenna system. It is a simple method to excite the cavity and to determine the quality factor Q. This Q measurement technique become very useful. The measurements are done by sweeping the

frequency and displaying the detected spectrum on the VNA monitor. The detected spectrum is modulated by a standing wave which originates in the cavity under test. Cavity resonances can be observed on the standing wave pattern. The background standing wave pattern varies with resonator orientation. The cavity is oriented in such a way so that a resonance occurs on a peak or minimum of the standing wave pattern. In this way the half maximum width of the resonance can be more accurately determined for the Q measurements. The cavity resonant frequency can also be determined by these measurements more accurately. The resonances can be identified separately and have sufficient frequency separation. The resonator Q factor determines the gyrotron operating characteristics, otherwise small cavity imperfections which are not traceable from visual inspection and the measurements would show that the Q of the cavity is very different from the design value. High power gyrotrons used for electron cyclotron heating of fusion plasmas requires low Q to minimize resonator wall loading. It is important to achieve the design value of Q of the resonator for obtaining the required performance of a particular gyrotron. The advantages of this method are (i) any resonator mode can be studied with the same experimental set-up, (ii) no mode convertors are required, (iii) the RF cavity resonator is not damaged in any way and can be applied to any type of resonator and (iv) the undesired modes are reduced in the radiation pattern of the cavity by adopting this technique for characterization of the same.
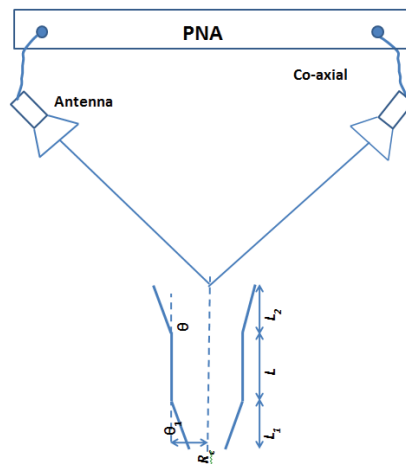

Fig. 4.15: Block diagram of "Non-destructive" method using antenna system.

4.5.3 Non-destructive external adaptor method

The external adapter is used for the excitation of the electric field inside the cavity in the non-destructive external adaptor method. An electric probe is inserted through 1mm diameter

hole at the center of the adapter for the excitation of TE mode. In this method electric probe works as a monopole antenna. Fig. 4.16 shows the experimental set up for the measurement of eigenfrequency (f) and the total quality factor (Q_T). The eigenfrequency is measured by the resonance on the VNA. The loaded quality factor is calculated by half power bandwidth method at -3 dB point. Table 4.4 show the quality factors values obtained from different methods and compared with the calculated values to a sastisfactory agreement.
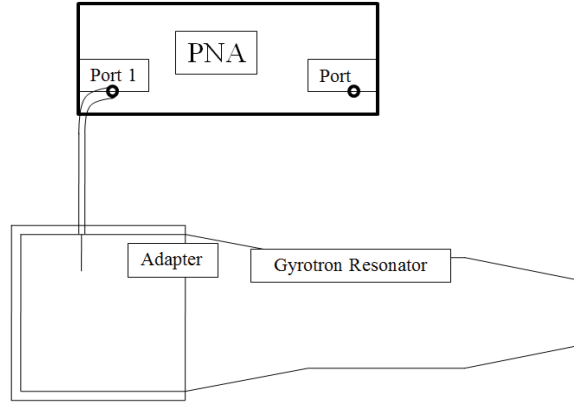

Fig. 4.16: The experimental set up for the non-destructive external adaptor method.

Table 4.4: Calculated and measured values of resonant frequency and quality factor for 42GHz Gyrotron excited for the TE$_{03}$ mode.

Destructive Method			
Calculated	**Measured**	**Calculated**	**Measured**
f (GHz)	f (GHz)	Q_{tot}	Q_{tot}
41.988	41.905	860	910
Non- destructive Horn antenna Method			
41.988	41.905	860	900
Non- destructive External Adapter Method			
41.988	41.75	860	910

4.6   Design of the RF Interaction Cavity for the 28 GHz Gyrotron

The MIG type electron gun designed and developed here for a 42GHz gyrotron is also found to be suitable for its use at another frequency gyrotron, namely, 28GHz gyrotron as discussed previously in Section 2.6 of Chapter 2. However, for this effective use of 42GHz MIG as 28GHz MIG, the operating mode and RF interaction cavity, cavity magnetic field, beam launching position, etc. are to be properly designed and verified at 28GHz.

Thus, at first, the operating mode and the cavity dimensions, magnetic field, etc. are obtained for a 28GHz gyrotron RF interaction cavity through the synthesis process (Section 4.2). Then the nonlinear analysis (Section 4.3) is used to design the RF interaction cavity parameters at 28GHz frequency. The operating mode is found to be suitable for the 28GHz gyrotron is $TE_{3,2}$ and for fundamental mode operation, with cavity magnetic field equal to 1.0T for beam voltage = 65kV and beam current = 10A. Figs. 4.17 and 4.18 present the typical results obtained by the generalized non-linear analysis code for the interaction cavity for use in 28GHz gyrotron using the MIG parameters of Section 2.5 of Chapter 2. Fig. 4.17 confirms energy transfer from the electron beams to the RF field while Fig. 4.18 shows the phase bunching of the gyrating electron beam for a 28GHz cavity. Total 32 beamlets are considered in the calculations. The results obtained from the non-linear theory confirm the interaction efficiency of 18.2%.
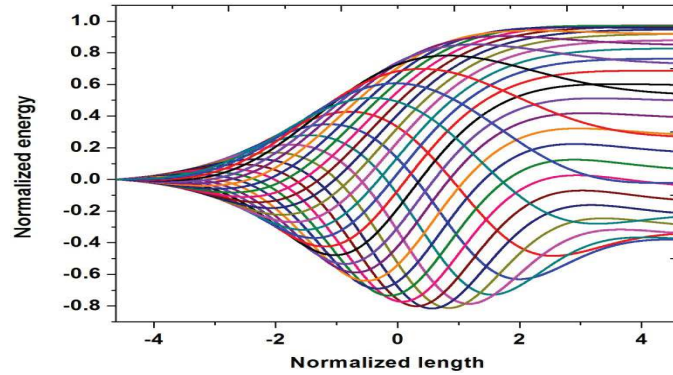

Fig. 4.17: Normalized energy with respect to the normalized phase for 28GHz gyrotron cavity.
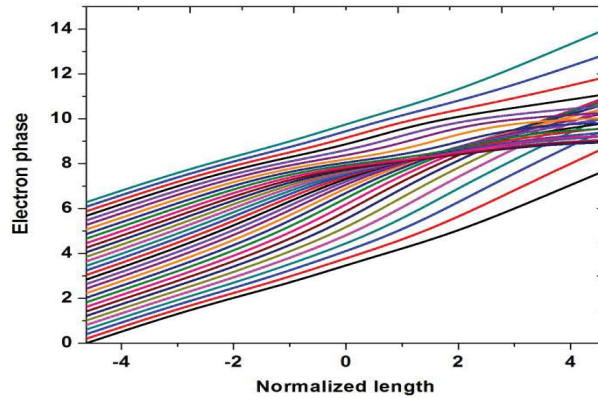

Fig. 4.18: Normalized length versus electron phase plot for 28 GHz gyrotron cavity.

The beam-wave interaction simulation is also performed using the Particle-In-Cell (PIC) code MAGIC for the 28GHz gyrotron. The interaction cavity geometry is generated in the cylindrical coordinate system and the Maxwell Centered FDTD algorithm has been implemented

in the simulations. The gyrating electron beam is launched at the first maxima of the operating mode $TE_{3,2}$ with a beam radius of 5.2 mm. Figs. 4.19 and 4.20 show the simulation results obtained from PIC code MAGIC. Fig. 4.19 shows the temporal growth of RF power and confirms the growth of more than 100kW of RF power. Fig. 4.20 shows the fast Fourier transform (FFT) frequency spectrum curve for the electric field in the designed interaction cavity. It can be easily concluded from Fig. 4.20 that a sharp peak of the electric field gain is appearing at 28 GHz frequency which confirms the interaction cavity oscillation at the desired 28GHz frequency. The optimized cavity geometrical and electron beam parameters are summarized in Table 4.5. It is of interest to mention that the results presented in Figs. 4.17-4.20 are based on the beam parameters shown in Table 4.5 and analytical computed interaction efficiency 18% while the PIC beam-wave simulation results estimate 17% interaction efficiency, a close agreement.
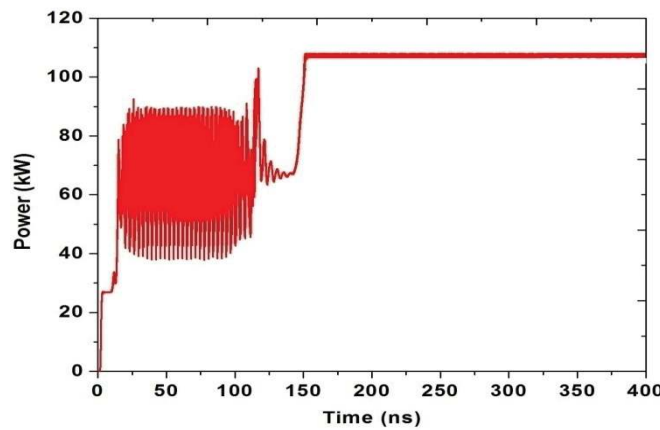

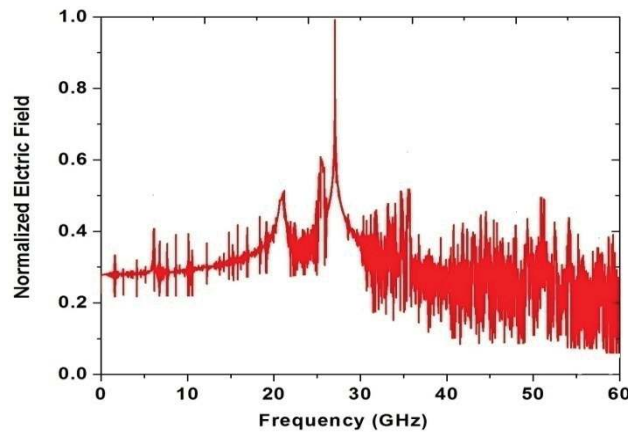**Fig. 4.19:** Temporal growth of RF power for 28 GHz gyrotron cavity.

Fig. 4.20: Frequency spectrum of a 28 GHz gyrotron cavity (beam voltage= 65kV, beam current= 10A, cavity magnetic field= 1.05T).

Table 4.5: Optimized interaction cavity geometrical and beam parameters.

Parameter	Value
Middle section length	60 mm
Middle section radius	13.5 mm
Input taper length	40 mm
Output taper length	60 mm
Input taper angle	2.5 degree
Output taper angle	3.5 degree
Beam radius	5. 2 mm
Beam voltage	65 kV
Beam current	10 A
Cavity magnetic field	1.05 T

4.7   Conclusion

The RF interaction cavity of the gyrotron is the main active region of the device where the interaction between the electron beam and the RF waves present in the cavity takes place which results in the RF signal growth responsible for large RF power output from this oscillator. The various aspects of the RF interaction cavity have been discussed in this Chapter 4. At first, the synthesis of the RF interaction cavity has been carried out to estimate the operating TE mode, resonant frequency, quality factor as well as the cavity dimensions. It has been established here that the TE_{03} is most suitable and effective operating mode with respect to various design parameters, such as, voltage depression, limiting current, power loss at the cavity wall, start oscillation current, coupling coefficient, etc.

To estimate the RF power growth for this 200 kW at 42 GHz operating frequency of the gyrotron where this RF cavity has to be integrated, a generalized nonlinear analysis is used. A Matlab based code has been written for the purpose using the various coupled nonlinear expression obtained through this nonlinear analysis for the gyrotron oscillator. This analysis has been used here to estimate and optimize the results for RF power output and device efficiency for the sake of more accurate performance estimation.

To further explore the designed device behavior, PIC simulation has also been done for the designed gyrotron using a commercially available code MAGIC. The code has been reconfigured for our device and a structure model has been made as per our designed structural and electrical parameters. The PIC simulation has been performed for both the electron beam absent case (cold condition) as well as for the beam present case (hot condition) of the designed device. The simulated results have been found to be in close agreement with those obtained through the nonlinear analysis of this device. This process confirms the validity of our device design as well as validates the efficacy of both the nonlinear analysis and the PIC simulation. This further helps us in confidence building in absence of previous experience in this area.

After gaining the confidence towards the device design, we further moved forward and got fabricated RF interaction cavity of the 42GHz 200kW gyrotron. Now, the experimental validations of fabricated gyrotron cavity have also been carried out through different characterization methods and found the comparable results with the analytical values.

It is to worth mentioning here that the use of the developed MIG type electron gun for the present 42GHz gyrotron has been studied for its direct incorporation in another gyrotron such as 28GHz gyrotron which is normally used for material processing application. Through analysis and optimization, the necessary cavity parameters have been obtained for 28GHz gyrotron with electron beam parameters of 42GHz gyrotron. It has been found that with new operating mode $TE_{3,2}$ along with the modified RF cavity dimensions, 100kW output power for 28GHz gyrotron can easily be achieved.